

NASA/TM—2001-210693



Aeroelastic Stability Computations for Turbomachinery

R. Srivastava, M.A. Bakhle, and T.G Keith, Jr.
University of Toledo, Toledo, Ohio

G.L. Stefko
Glenn Research Center, Cleveland, Ohio

Prepared for the
International Forum on Aeroelasticity and Structural Dynamics
cosponsored by the CEAS, AIAA, and AIAE
Madrid, Spain, June 5–7, 2001

National Aeronautics and
Space Administration

Glenn Research Center

June 2001

Acknowledgments

This work was supported by the Advanced Subsonic Technology and the Ultra Efficient Engine Technology Projects through a grant from NASA Glenn Research Center.

Available from

NASA Center for Aerospace Information
7121 Standard Drive
Hanover, MD 21076

National Technical Information Service
5285 Port Royal Road
Springfield, VA 22100

Available electronically at <http://gltrs.grc.nasa.gov/GLTRS>

AEROELASTIC STABILITY COMPUTATIONS FOR TURBOMACHINERY

R. Srivastava, M.A. Bakhle, and T.G. Keith, Jr.

University of Toledo
Toledo, Ohio

G.L. Stefko

National Aeronautics and Space Administration
Glenn Research Center
Cleveland, Ohio

Abstract. This paper describes an aeroelastic analysis program for turbomachines. Unsteady Navier-Stokes equations are solved on dynamically deforming, body fitted, grid to obtain the aeroelastic characteristics. Blade structural response is modeled using a modal representation of the blade and the work-per-cycle method is used to evaluate the stability characteristics. Non-zero inter-blade phase angle is modeled using phase-lagged boundary conditions. Results obtained showed good correlation with existing experimental, analytical and numerical results. Numerical analysis also showed that given the computational resources available today, engineering solutions with good accuracy are possible using higher fidelity analyses.

1 INTRODUCTION

Aeroelastic problems contribute significantly to the development and maintenance costs of aircraft engines. In turbomachinery, both flutter and synchronous vibration can cause blade failures. Flutter problems, usually detected during the design phase, cause significant program delays and cost overruns. Numerical methods are being developed to help design flutter free turbomachinery components.

Several methods have been developed for the prediction of aeroelastic characteristics of turbomachines with various degrees of fidelity. Aeroelastic analyses based on energy exchange between vibrating blades and the surrounding fluid, have been reported for turbomachines using semi-analytical methods (Lane and Friedman,¹ Smith²), linearized methods (Hall and Clark,³ Verdon⁴), Euler methods (He,⁵ Gerolymos and Vallet,⁶ Bakhle, et al.⁷) and viscous methods (Giles and Haines,⁸ Siden,⁹ He and Denton¹⁰). A limited number of coupled aeroelastic analyses of turbomachine configurations have also been reported.¹¹⁻¹³ Williams, Cho, and Dalton¹¹ used a linear panel method to solve the eigenvalue problem. Gerolymos,¹² and Srivastava and Reddy¹³ solved the coupled aeroelastic equations based on an inviscid aerodynamic analysis. The majority of the methods are either analytical, applicable to two-dimensional geometry and/or ignore the viscous effects.

The objective of the present effort is to report an aeroelastic analysis program based on Navier-Stokes equations and its application to turbomachinery components. The results obtained are compared to those obtained from a two-dimensional linear method which solves the linear, compressible, potential flow equation,² to those obtained from a three-dimensional linearized Euler analysis,¹⁴ and to existing experimental data from a linear turbine blade cascade¹⁵ and a transonic fan configuration.¹⁶

2 THE TURBO-AE CODE

The aeroelastic solver TURBO-AE is briefly described in this section. The solver can model multiple blade rows undergoing harmonic oscillations with arbitrary inter-blade phase angles (IBPAs). It is based on a Navier-Stokes unsteady aerodynamic solver for internal flow calculations of axial flow turbomachinery components TURBO.^{17,18} Viscous effects are modeled using the Reynolds-averaged Navier-Stokes equations. The Baldwin-Lomax or two-equation $k-\epsilon$ turbulence model is used for closure. The aerodynamic equations are solved using a finite volume scheme. Flux vector splitting is used to evaluate the flux Jacobians on the left-hand side. The right-hand side fluxes are discretized using the high order Total Variation Diminishing (TVD) scheme based on Roe's flux difference splitting. Newton subiterations are used at each time-step to maintain accuracy. Symmetric Gauss-Seidel iterations are applied to the discretized equations for improved convergence.

The aeroelastic characteristics of the rotor are obtained by calculating the energy exchange between the vibrating blade and its surrounding fluid. If work on the blade is positive, this indicates instability. The aeroelastic analysis is carried out by first obtaining the "steady" aerodynamic solution for a given operating condition. The blades are then forced into a prescribed harmonic motion (specified mode, frequency, and IBPA) to calculate the unsteady aerodynamic response and work-per-cycle. The blade motion is simulated using a dynamic grid deformation technique. Phase-lagged boundary conditions are used to calculate the non-zero IBPA vibrations, which eliminates the need to model multiple blade passages.

3 RESULTS AND DISCUSSION

Results were obtained for a flat plate helical fan, a linear cascade of turbine blades and a transonic fan configuration. These results are compared with existing analytical, numerical or experimental data.

Flat Plate Helical Fan: The helical fan geometry consists of 24 unswept, untapered, zero thickness, twisted flat plate blades enclosed within a rigid cylindrical duct of infinite length with no tip gap. The fan's operating condition was set at a relative inflow Mach number of 0.7 and zero incidence at midspan with a 0.495 axial Mach number.

Linear Turbine Cascade: A cascade of turbine blades with large flow turning (112 deg) was tested for several expansion ratios, exit Mach numbers and IBPAs.¹⁵ The experimental facility consisted of a cascade comprising of five airfoil sections in a stator configuration. In TURBO-AE the linear cascade was modeled as an annular cascade with 96 blades, with a 0.98 hub-tip-ratio, and a tip radius of 21.4625 inches. These parameters were selected to match the solidity of the test cascade at midchord. The analysis was carried out for the measured condition of 2.731 expansion ratio with an exit flow Mach number of 1.25.

Transonic Fan: A scale model of an experimental transonic fan designated Quiet High Speed Fan (QHSF), with 22 blades, design rpm of 15444, relative tip Mach number of 1.4, and mass flow of 98.89 Kg/s was tested in a rig. The fan fluttered at part speed in the first bending mode.¹⁶ Results are presented for 90% speed at several back pressures and IBPAs.

3.1 Flat Plate Helical Fan

Results obtained for the flat plate helical fan configuration and an inviscid analysis using TURBO-AE are presented in this section. The advantage of this configuration and flow condition is that the flow is subsonic and well behaved, and a large hub to tip ratio allows modeling a 2-D flowfield that can be closely approximated at the midspan of the blade. This allows a comparison with results obtained from an analytical solution using linear theory.² Montgomery and Verdon¹⁵ using a linearized Euler analysis have also analyzed this particular configuration. Since this configuration is a flat plate with zero thickness at zero incidence, there is no steady load on the blade. The unsteady results for two different configurations –0 deg IBPA for pitching motion and 180 deg IBPA for plunging motion are shown in Figs. 1 and 2. The variation of the unsteady pressure difference with chord at midspan for pitching motion is compared with linear theory² and linearized Euler analysis¹⁵ in Fig. 1 and for the plunging motion in Fig. 2.

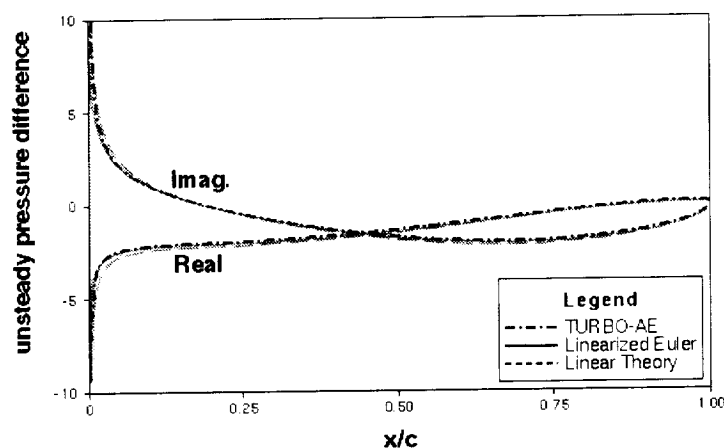


Figure 1. Unsteady pressure difference variation with chord at midspan for 0 deg IBPA pitching oscillations

Excellent agreement is realized among the three methods. Figure 3 shows the variation of the unsteady pressure difference with chord for several phase angles for the pitching motion. The variation for the plunging motion is shown in Figure 4. These results are for the first harmonic of the unsteady blade surface pressure difference at the midspan location. The results obtained from TURBO-AE are compared with results obtained from the linear theory² in these figures. Good agreement is obtained over most of the range except in the neighborhood of acoustic resonance (cut-on and cut-off regions). Acoustic resonance occurs at phase angles of 107.3 and 330.6 deg. The phase angles between these resonances are associated with subresonant¹⁹ (cut-off) conditions in which all disturbances attenuate away from the cascade. No disturbances propagate upstream or downstream under subresonant conditions. The phase angles between 0 and 107.3 deg. and between 330.6 and 360 deg. are associated with super-resonant (cut-on) conditions in which at least one disturbance propagates in either the far upstream or downstream direction.

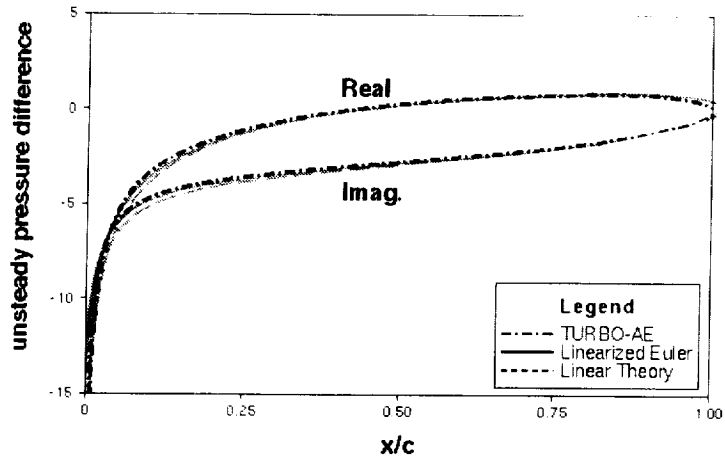


Figure 2. Unsteady pressure difference variation with chord at midspan for 180 deg IBPA plunging oscillations

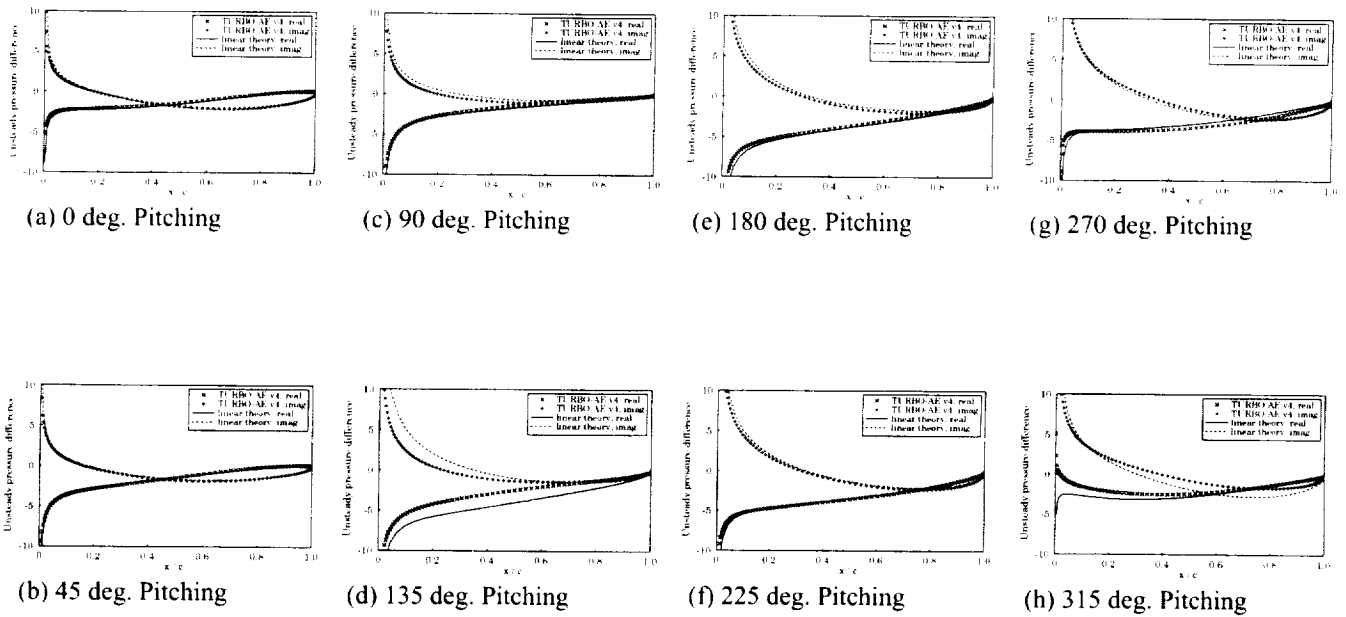


Figure 3. Unsteady pressure difference (first harmonic) for pitching motion

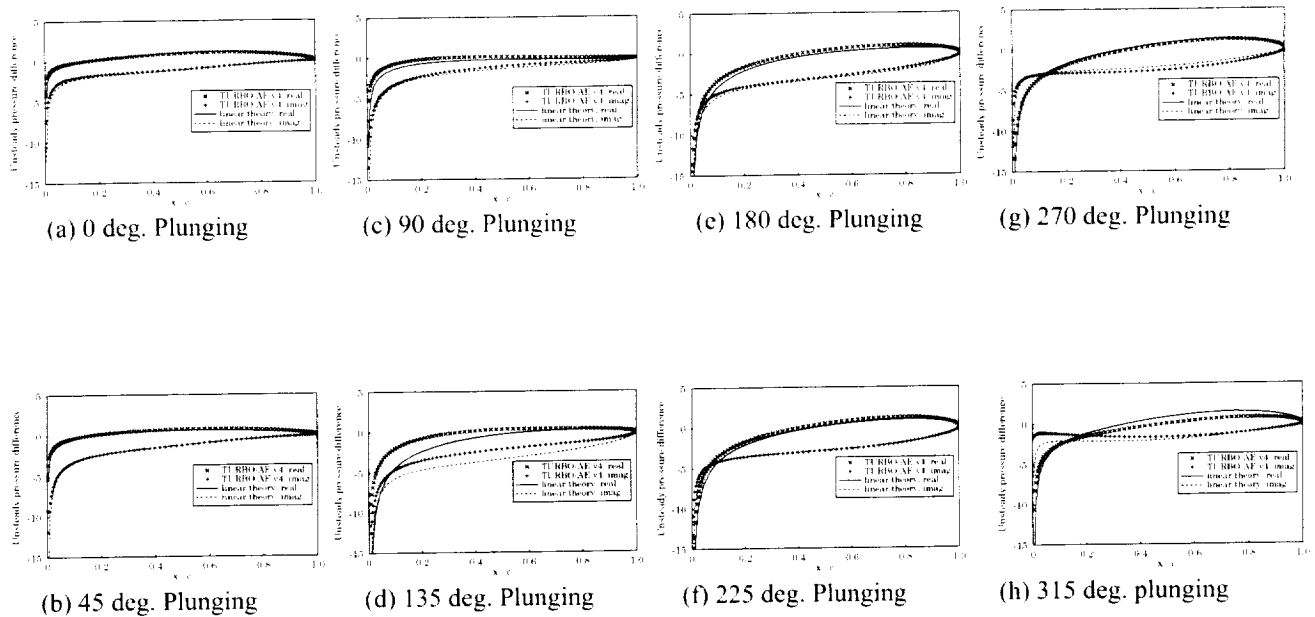


Figure 4. Unsteady pressure difference (first harmonic) for plunging motion

Figure 4 shows the comparison with linear theory² for plunging blade motion. The overall level of agreement with linear theory is good. Once again deviations are observed close to the acoustic resonances, as for pitching. The level of agreement was found to be better for pitching motion than for plunging motion.

3.2 Linear Turbine Cascade

Results for the linear turbine cascade configuration are presented next. A 2.713 expansion ratio provided a test case in which the cascade inlet velocity was subsonic (0.52 Mach), while the exit velocity was supersonic (1.25 Mach). Predictions for the steady blade surface pressure distribution, obtained from TURBO-AE, are compared to measurements in Fig. 5. Excellent agreement with the measured values is obtained over most of the blade surface. However, in the leading edge region on the pressure surface and the aft section of the suction surface small differences are apparent. In the leading edge region, a separation bubble was observed, which is not captured very accurately in the analysis. An expansion fan originating from the trailing edge of the adjacent blade impinges on the aft 30 percent of the suction surface. Because of relatively coarse grid in the blade passage the expansion fan impacts the suction surface a little upstream from that measured.

The unsteady pressure calculated for the cascade is shown in Figs. 6 and 7 for a forced blade motion of 180 deg IBPA and 340 Hz vibration frequency. Comparison of calculated and measured pressure amplitude variation with chord is shown in Fig. 6. The phase comparison is shown in Fig. 7. Good comparison is seen for the unsteady pressure variation with chord. The phase comparison, which is more important in flutter prediction, shows better agreement than pressure amplitude. The unsteady pressure measurements were sparse on the suction surface since a transducer located at the 30% chord location was not working. In the trailing edge region of the suction surface the code missed the measured increase in unsteady pressure magnitude aft of the point where the trailing edge expansion fan intersects the blade.

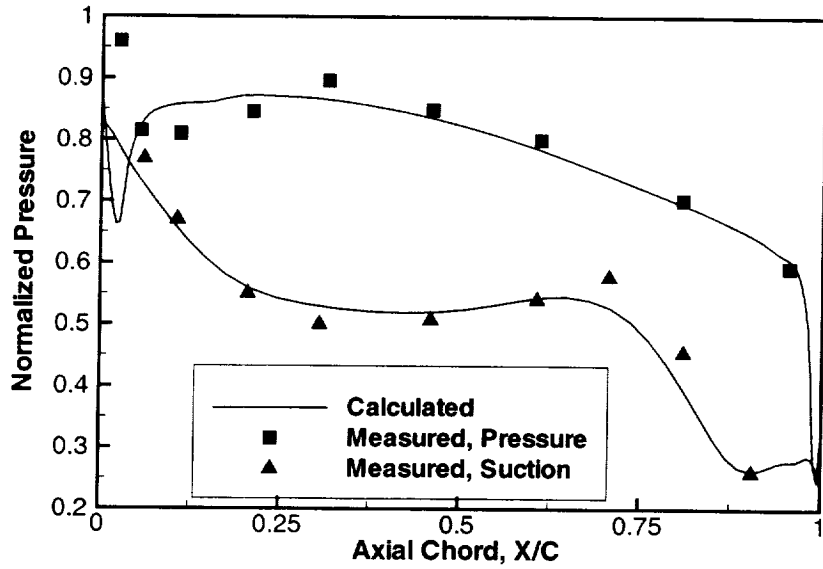


Figure 5. Comparison of steady blade loading for the turbine cascade at an expansion ratio of 2.713

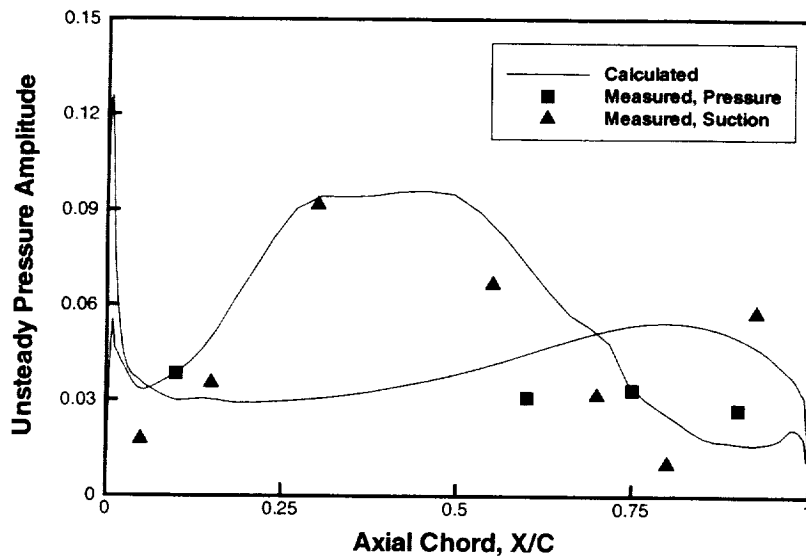


Figure 6. Comparison of unsteady pressure response amplitude for the turbine cascade vibrating in a torsional mode at 340 Hz, 180° IBPA, and 2.713 expansion ratio

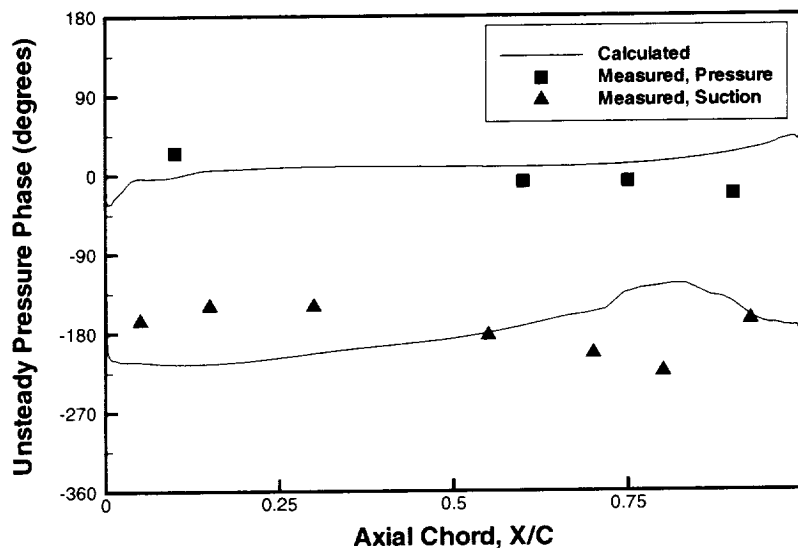


Figure 7. Comparison of unsteady pressure response phase for the turbine cascade vibrating in a torsional mode at 340 Hz, 180° IBPA, and 2.713 expansion ratio

3.3 Transonic Fan

The analysis was next applied to calculate the aeroelastic characteristics of the QHSF. The results presented here are for the 90% speed line. Experiments showed blade flutter in the first natural mode (natural frequency 351 Hz) for 32.73 IBPA (2 Nodal Diameter forward travelling wave).¹⁶ The calculated time history of mass flow is shown in Fig. 8 for flow with and without blade vibration for back pressure of 16.2 pounds per square inch (psi). The “steady” flow results or results for no blade vibrations show a time dependency, although the mean mass flow is constant. A closer examination of the flowfield revealed flow separation and subsequent shedding of the vortex in the vicinity of the hub in the aft section of the blade. Increasing the back pressure lengthened the region of separation and also moved it further upstream. Also shown on this figure is the variation of mass flow after the blades are forced to undergo prescribed vibration of 180 deg IBPA at 351 Hz. Because of the mean flow unsteadiness, one needs to ensure that the blade vibration amplitude is large enough so as to minimize the impact of mean flow unsteadiness on the unsteadiness due to blade vibrations. It can be seen from Fig. 8 that for the vibration amplitude chosen for the analysis, the unsteadiness due to blade vibration is at least an order of magnitude larger than the mean flow unsteadiness. It can also be seen that the flow converges to periodicity in roughly 10 blade vibration cycles.

Figure 9 shows the aerodynamic damping calculated for several different back pressures and IBPAs. For lower back pressures, the least stable IBPA was found to be 0 deg. However, as the back pressure was raised moving the fan operating condition towards the stall line, the 32.73 deg IBPA (2 nodal diameter forward travelling wave) became least stable. Flutter was observed in the wind tunnel for 32.73 deg IBPA. The calculated variation of aerodynamic damping with back pressure is shown in Fig. 10 for 32.73 deg IBPA. As may be seen in the figure, as the back pressure is increased, the aerodynamic damping decreases rapidly, dropping to approximately 0.2% of critical damping for the back pressure of 16.4 psi. For the grid used, and because of computational constraints, the highest back pressure analyzed was 16.4 psi. Increasing the back pressure above 16.4 psi for 90% speed resulted in stalled flow with large separation on the

suction surface in the mid section of the blade. This separation was found to be shock induced and prevented a steady mean flow from which the blade vibration analysis could be carried out. These results indicate that the 32.73 IBPA is the least stable IBPA for first natural mode, as observed in experiments, and that the aerodynamic damping is rapidly decreasing with increasing back pressure. It can be easily extrapolated from Fig. 10 that further increase in the back pressure would result in a negative aerodynamic damping indicating flutter.

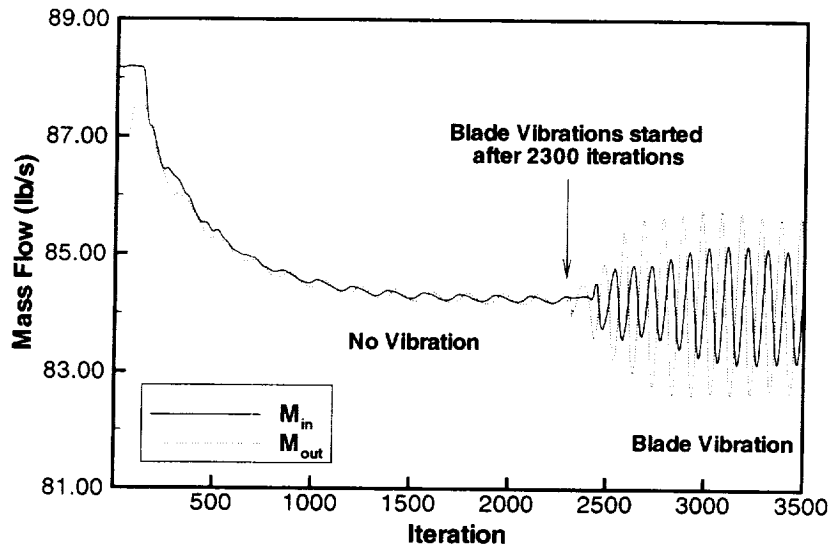


Figure 8. Variation of mass flow for the transonic fan, with and without blade vibration

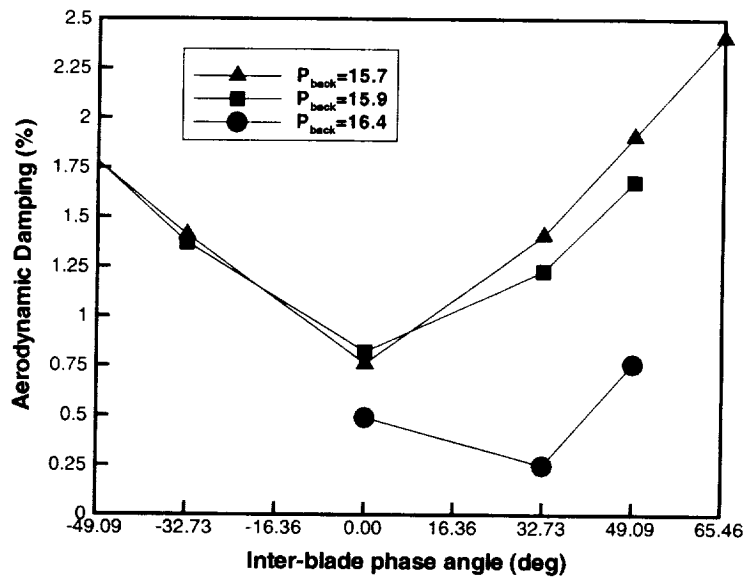


Figure 9. Variation of aerodynamic damping with back pressure and IBPA for the transonic fan with forced blade vibration in the first natural mode at the natural frequency of 351 Hz

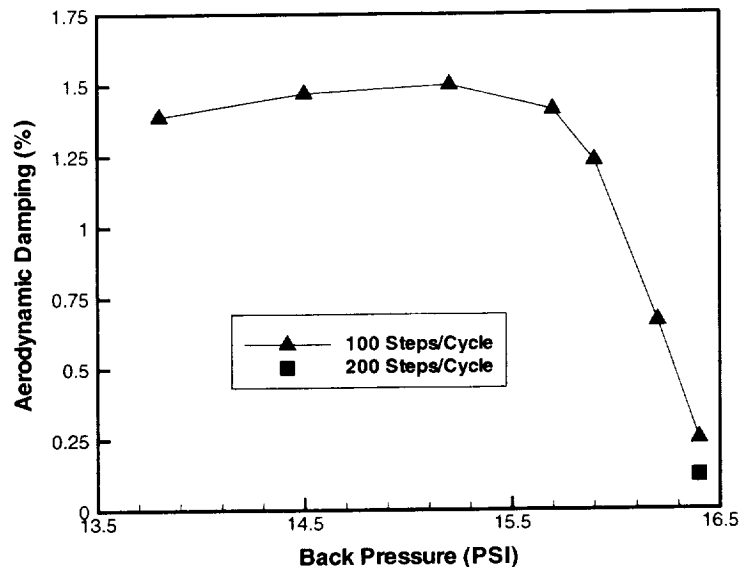


Figure 10. Variation of aerodynamic damping for 16.4 PSI back pressure. Forced vibration in the first natural mode at 351 Hz and 32 deg IBPA

For the back pressure of 16.4 psi, the experiment showed flutter, whereas the analysis predicted the fan to be marginally stable. In the analysis, the 100% speed blade shape and blade modal properties were used at the 90% speed. Changes in rotational speed impact the geometry by affecting tip-gap, blade natural frequency, and blade shape or more specifically twist distribution. These factors may have contributed to the over prediction of aerodynamic damping. It has been reported that tip-gap may have significant impact on stability.²⁰ The analyses used a uniform value of tip-gap which is based on measurements made during testing. However, the axial distribution of tip-gap and the accuracy of the measurements are not known. Further, a sensitivity analysis did not show a strong influence of natural frequency on aerodynamic damping.

Analysis was also performed at the second natural vibration mode, which was stable in the experiment. The aerodynamic damping calculated was much higher than those for the first mode, indicating the second mode to be more stable than the first mode. These results clearly show that the analysis successfully calculates the natural mode and IBPA of instability identifying the flutter characteristics of the QHSF.

4 CONCLUDING REMARKS

An aeroelastic analysis program based on the Navier-Stokes equation has been reported and applied to several turbomachinery components in this study. The calculated unsteady aerodynamic pressure variations are compared with existing numerical, analytical and experimental results for a fan and a turbine configuration. Good comparisons between analytical and numerical results were found for a fan-type geometry, with the exception being the neighborhood of acoustic resonances. Comparisons with the more challenging case of a turbine

configuration was also good in general. The unsteady aerodynamic characteristics obtained for the turbine configuration compared well with measured data. The grid used was not able to capture all the details of flow separation resulting in some differences in the calculated pressure. The important characteristics of phase variation, which determines the flutter characteristics, were captured well. Increasing the grid density and using smaller time-steps in time march can further improve the details of the calculated results.

Calculated variations of aerodynamic damping with back pressure and IBPA is presented for a transonic fan at a condition where flutter occurred during testing. Although a negative aerodynamic damping was not calculated, the analysis yielded some good results and trends. The analysis correctly predicted the mode and IBPA of flutter. Also, the trend for calculated aerodynamic damping clearly indicated a negative aerodynamic damping would result with further increasing the back pressure. Unfortunately, the analysis showed a stalled flow field would emerge for any further increase of the back pressure. Although flow separation was captured along with vortex shedding, deep blade stall posed a numerical problem.

The results presented here required roughly 4 to 5 days on a SGI Octane per analysis, these computational times are within the realm of engineering analyses. Moreover, these results indicate that the aeroelastic analysis program presented here is accurate and fast enough to be used in engineering applications for aeroelastic analysis of modern turbomachinery components.

5 REFERENCES

- [1] Lane, F. and Friedman, M., "Theoretical Investigation of Subsonic Oscillating Blade-Row Aerodynamics," NACA TN 4136, 1958.
- [2] Smith, S.N., "Discrete Frequency Sound Generation in Axial Flow Turbomachines," R&M 3709, British Aeronautical Research Council, London, England, UK, 1972.
- [3] Hall, K.C., Clark, W.S., "Linearized Euler Predictions of Unsteady Aerodynamic Loads in Cascades," *AIAA Journal*, vol. 31, pp. 540–550, 1993.
- [4] Verdon, J.M., "Unsteady Aerodynamic Methods for Turbomachinery Aeroelastic and Aeroacoustic Applications," *AIAA Journal*, vol. 31, no. 2, pp. 235–250, 1993.
- [5] He, L., "An Euler Solution for Unsteady Flows Around Oscillating Blades," *ASME Journal of Turbomachinery*, vol. 112, no. 4, pp. 714–722, 1989.
- [6] Gerolymos, G.A., and Vallet, I., "Validation of 3-D Euler Methods for Vibrating Cascade Aerodynamics," ASME Paper 94–GT–294, 1994.
- [7] Bakhle, M.A., Srivastava, R., Keith, T.G. Jr., Stefko, G.L., "A 3D Euler/Navier-Stokes Aeroelastic Code for Propulsion Applications," AIAA Paper No. 97–2749, 1997.
- [8] Giles, M., Haines, R., "Validation of a Numerical Method for Unsteady Flow Calculations," ASME Paper 91–GT–271, 1991.
- [9] Siden, L.D.G., "Numerical Simulation of Unsteady Viscous Compressible Flows Applied to a Blade Flutter Analysis," ASME Paper No. 91–GT–203, 1991.

- [10] He, L. and Denton, J.D., "Three Dimensional Time Marching Inviscid and Viscous Solutions for Unsteady Flows Around Vibrating Blades," *ASME Journal of Turbomachinery*, vol. 116, pp. 469–476, 1994.
- [11] Williams, M.H., Cho, J., and Dalton, W.N., "Unsteady Aerodynamic Analysis of Ducted Fans," *Journal of Propulsion and Power*, vol. 7, no. 5, pp. 800–804, 1991.
- [12] Gerolymos, G.A., "Coupled 3-D Aeroelastic Stability Analysis of Bladed Disks," ASME Paper No. 92–GT–171, 1992.
- [13] Srivastava, R. and Reddy, T.S.R., "Comparative Study of Coupled-Mode Flutter-Analysis Methods for Fan Configurations," *Journal of Propulsion and Power*, vol. 15, no. 3, pp. 447–453, 1999.
- [14] Montgomery, M.D. and Verdon, J. M., "A Three-Dimensional Linearized Unsteady Euler Analysis for Turbomachinery Blade Rows," NASA CR–4770, 1997.
- [15] Rothrock, M.D., Jay, R.L., and Riffel, R.E., "Time Variant Aerodynamics of High-Turning Blade Elements," ASME Paper No. 81–GT–123, 1981.
- [16] Fite, B.E., Private Communications, NASA Glenn Research Center, January 2001.
- [17] Chen, J.P., "Unsteady Three-Dimensional Thin-Layer Navier-Stokes Solutions for Turbomachinery in Transonic Flow," Ph. D. Dissertation, Mississippi State University, 1991.
- [18] Janus, J.M., "Advanced 3-D CFD Algorithm for Turbomachinery," Ph. D. Dissertation, Mississippi State University, Mississippi, 1989.
- [19] Verdon, J.M., "The Unsteady Flow in the Far Field of an Isolated Blade Row," *Journal of Fluids and Structures*, vol. 3, no.2, pp. 123–149, 1989.
- [20] Srivastava, R. and Reddy, T.S.R., "Aeroelastic Analysis of Ducted Rotors," Proceedings of International Symposium on Computational Fluid Dynamics in Aeropropulsion, San Francisco, AD-vol. 49, pp. 1–9, November 1995.

REPORT DOCUMENTATION PAGE

Form Approved
OMB No. 0704-0188

Public reporting burden for this collection of information is estimated to average 1 hour per response, including the time for reviewing instructions, searching existing data sources, gathering and maintaining the data needed, and completing and reviewing the collection of information. Send comments regarding this burden estimate or any other aspect of this collection of information, including suggestions for reducing this burden, to Washington Headquarters Services, Directorate for Information Operations and Reports, 1215 Jefferson Davis Highway, Suite 1204, Arlington, VA 22202-4302, and to the Office of Management and Budget, Paperwork Reduction Project (0704-0188), Washington, DC 20503.

1. AGENCY USE ONLY (<i>Leave blank</i>)	2. REPORT DATE June 2001	3. REPORT TYPE AND DATES COVERED Technical Memorandum	
4. TITLE AND SUBTITLE Aeroelastic Stability Computations for Turbomachinery		5. FUNDING NUMBERS WU-714-03-50-00	
6. AUTHOR(S) R. Srivastava, M.A. Bakhle, T.G Keith, Jr., and G.L. Stefko			
7. PERFORMING ORGANIZATION NAME(S) AND ADDRESS(ES) National Aeronautics and Space Administration John H. Glenn Research Center at Lewis Field Cleveland, Ohio 44135-3191		8. PERFORMING ORGANIZATION REPORT NUMBER E-12821	
9. SPONSORING/MONITORING AGENCY NAME(S) AND ADDRESS(ES) National Aeronautics and Space Administration Washington, DC 20546-0001		10. SPONSORING/MONITORING AGENCY REPORT NUMBER NASA TM-2001-210693	
11. SUPPLEMENTARY NOTES Prepared for the International Forum on Aeroelasticity and Structural Dynamics cosponsored by the CEAS, AIAA, and AIAE, Madrid, Spain, June 5-7, 2001. R. Srivastava, M.A. Bakhle, and T.G Keith, Jr., University of Toledo, Toledo, Ohio 43606; and G.L. Stefko, NASA Glenn Research Center. Responsible person, G.L. Stefko, organization code 5930, 216-433-3920.			
12a. DISTRIBUTION/AVAILABILITY STATEMENT Unclassified - Unlimited Subject Categories: 07 and 02 Available electronically at http://gltrs.grc.nasa.gov/GLTRS This publication is available from the NASA Center for AeroSpace Information. 301-621-0390.		12b. DISTRIBUTION CODE	
13. ABSTRACT (<i>Maximum 200 words</i>) This paper describes an aeroelastic analysis program for turbomachines. Unsteady Navier-Stokes equations are solved on dynamically deforming, body fitted, grid to obtain the aeroelastic characteristics. Blade structural response is modeled using a modal representation of the blade and the work-per-cycle method is used to evaluate the stability characteristics. Nonzero interblade phase angle is modeled using phase-lagged boundary conditions. Results obtained showed good correlation with existing experimental, analytical, and numerical results. Numerical analysis also showed that given the computational resources available today, engineering solutions with good accuracy are possible using higher fidelity analyses.			
14. SUBJECT TERMS Turbomachinery; Flutter; Analysis; Navier-Stokes; Three-dimensional			15. NUMBER OF PAGES 17
			16. PRICE CODE
17. SECURITY CLASSIFICATION OF REPORT Unclassified	18. SECURITY CLASSIFICATION OF THIS PAGE Unclassified	19. SECURITY CLASSIFICATION OF ABSTRACT Unclassified	20. LIMITATION OF ABSTRACT



